Journal of Biomedical Optics

SPIEDigitalLibrary.org/jbo

Optical detection of carotenoid antioxidants in human bone and surrounding tissue

Igor V. Ermakov
Maia R. Ermakova
Thomas D. Rosenberg
Werner Gellermann

SPIE

Optical detection of carotenoid antioxidants in human bone and surrounding tissue

Igor V. Ermakov,[a] Maia R. Ermakova,[b] Thomas D. Rosenberg,[c] and Werner Gellermann[a]
[a]University of Utah, Department of Physics and Astronomy, Salt Lake City, Utah 84112
[b]Image Technologies, Inc., 419 Wakara Way, Suite 209, Salt Lake City, Utah 84108
[c]The Orthopedic Clinic at Park City, 900 Round Valley Drive, Suite 100, Park City, Utah 84060

Abstract. Carotenoids are known to play an important role in health and disease state of living human tissue based on their antioxidant and optical filtering functions. In this study, we show that carotenoids exist in human bone and surrounding fatty tissue both in significant and individually variable concentrations. Measurements of biopsied tissue samples with molecule-specific Raman spectroscopy and high-performance liquid chromatography reveal that all carotenoids that are known to exist in human skin are also present in human bone. This includes all carotenes, lycopene, β-cryptoxanthin, lutein, and zeaxanthin. We propose quantitative reflection imaging as a noncontact optical method suitable for the measurement of composite carotenoid levels in bone and surrounding tissue exposed during open surgeries such as total knee arthroplasty, and as a proof of concept, demonstrate carotenoid measurements in biopsied bone samples. This will allow one to establish potential correlations between internal tissue carotenoid levels and levels in skin and to potentially use already existing optical skin carotenoid tests as surrogate marker for bone carotenoid status. [DOI: 10.1117/1.JBO.18.11.117006]

Keywords: bone; carotenoids; knee surgery; Raman spectroscopy; reflection spectroscopy.

Paper 130564R received Aug. 9, 2013; revised manuscript received Sep. 25, 2013; accepted for publication Oct. 11, 2013; published online Nov. 8, 2013.

1 Introduction

Carotenoids are thought to play an important role in health and disease state of human tissue. Based on their antioxidant and optical filtering functions,[1] they may protect against various cancers,[2–5] cardiovascular disease,[6] macular degeneration,[7] and all-cause mortality.[8] In human skin, the composite carotenoid score can serve as an objective biomarker for fruit and vegetable intakes[9] and maybe even as an integrative biomarker of health,[10] since many dietary carotenoid species are accumulated in this tissue. These include, in order of decreasing concentrations, β-carotene, lycopene, lutein, α-carotene, β-cryptoxanthin, and zeaxanthin. The skin carotenoid levels can be rapidly and noninvasively assessed with optical methods in clinical as well as in field settings, making it possible to investigate correlations between fruit and vegetable intakes and health outcomes in large populations.[10]

In this article, we explore the presence of carotenoids and their potential optical detection in human bone and surrounding tissue. Bone is a living, dynamic, connective tissue which protects various organs, provides rigidity to the human skeleton, produces all blood cells, generates osteocalcin, and stores minerals for key biochemical processes. The optimal health and homeostasis of bone involve a dynamic balance between bone formation and resorption as well as a multitude of biochemical reactions necessary for life. This balance requires an intimate relationship with the environment, particularly as it relates to the food intake.

Indirect previous studies have already hinted at a potential beneficial role of carotenoids in bone health. Using bone tissue cultures *in vitro*, β-cryptoxanthin has been linked to the stimulation of bone-forming osteoblasts and to the inhibition of osteoclastic bone resorption, thereby increasing bone mass.[11] Epidemiological studies have suggested that high intakes of vegetables and fruits reduce the risk of osteoporosis, that carotenoid antioxidants are beneficial micronutrients for the maintenance of normal bone metabolism, that serum levels are associated with bone mineral density in postmenopausal women,[12] and that total carotenoid and lycopene intakes have a protective effect on hip fracture.[13]

Carotenoids absorb strongly in the blue-green wavelength region, and at high tissue concentrations, they are recognizable by the yellowish color they impart on the living human tissue. Long-term visual observations of the appearance of bone and connective tissue, exposed during open-knee implant surgery, by one of the authors (TDR) suggest that the integration/ingrowth capabilities of spongy femoral and tibial bones following total knee joint replacement correlate with the strength of a yellowish coloration of the bone and surrounding fatty tissue, which can be speculated to be due to the presence of carotenoids. Potentially, a strong correlation could exist between tissue carotenoid levels, healing responses after surgeries, and general bone health.

Examples for the differing visual appearances of flat femoral spongy bone surfaces prepared for the insertion of artificial knee joints in two patients are shown in Fig. 1. The photograph in the upper panel shows a femoral bone surface with a relatively healthy internal bone structure and exhibits a strong yellow coloration. The photograph in the lower panel shows the cut surface

Address all correspondence to: Werner Gellermann, University of Utah, Department of Physics and Astronomy, Salt Lake City, Utah 84112. Tel: 801 581-5222; Fax: 801-581-4801; E-mail: werner@physics.utah.edu

0091-3286/2013/$25.00 © 2013 SPIE

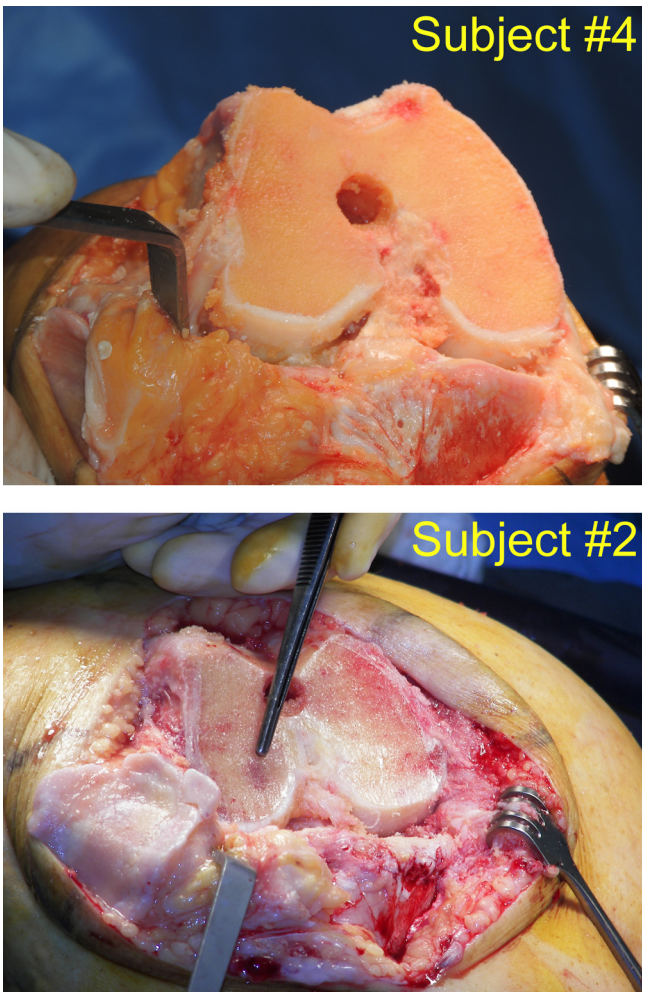

Fig. 1 Photographs of exposed femoral bone surfaces and surrounding tissue prepared for total knee replacement surgery. Upper panel: relatively healthy bone with surface featuring strong yellow coloration. Lower panel: bone with severe pathologies featuring pale yellow coloration.

of the distal femur having various pathologies (compromised structure, cysts, inflammation, and areas of locally reduced densities) and exhibits a relatively pale coloration. Both photographs were obtained during surgery under similar lighting and recording conditions. The difference in the yellowness of the exposed bone and fatty tissue in the two patients suggests a significant difference in tissue carotenoid levels.

Motivated by these observations, we investigated the composition and relative abundance of carotenoids in knee tissue, demonstrated the possibility to detect the composite carotenoid score optically with resonance Raman and reflection spectroscopies, and discussed skin carotenoid measurements as a potential surrogate marker for bone carotenoid status.

2 Experimental Results

2.1 *Resonance Raman Spectroscopy*

To prove the existence of carotenoids in bone and surrounding tissue, we first employed resonance Raman spectroscopy (RRS), which has emerged as a highly molecule-specific methodology for the noninvasive optical detection of carotenoids in the living human retina and in skin.[14–16] In bone research, Raman spectroscopy has already proven to be a valuable tool for the measurement of mineral composition.[17,18]

Wedge-shaped bone samples biopsied during total knee arthroplasty were prepared with at least one flat surface for optical interfacing. All samples were obtained from a standard bone cut (resection) at the postero-lateral femoral condyle during total knee implant surgery while under strict tourniquet control of bleeding. Each sample was placed into a sterile plastic cup, capped, and refrigerated within 30 to 60 min of excision. The biopsy site was selected because it appears uninvolved in the osteoarthritic degradation affecting diseased areas of the knee joint, namely the medial weight-bearing compartment and the patella-femoral compartment. As a consequence, it reflects more nearly the undiseased bone condition. In approximately 50% of all cases, samples were obtained from athletically active patients suffering from posttraumatic or secondary osteoarthritis.

After short storage at ice temperature, samples were warmed up to room temperature and placed in direct contact with the window of the light delivery and collection module of the RRS instrument. As an excitation source, an argon laser was used that generated ~10 mW power at 488 nm over a beam spot size of ~2 mm at the bone surface. The RRS spectra were recorded with a CCD-coupled grating spectrograph and displayed on a computer monitor. Representative bone spectra are shown in Fig. 2, where Fig. 2(a) shows the raw bone emission spectrum as a strong, spectrally broad, "autofluorescence"

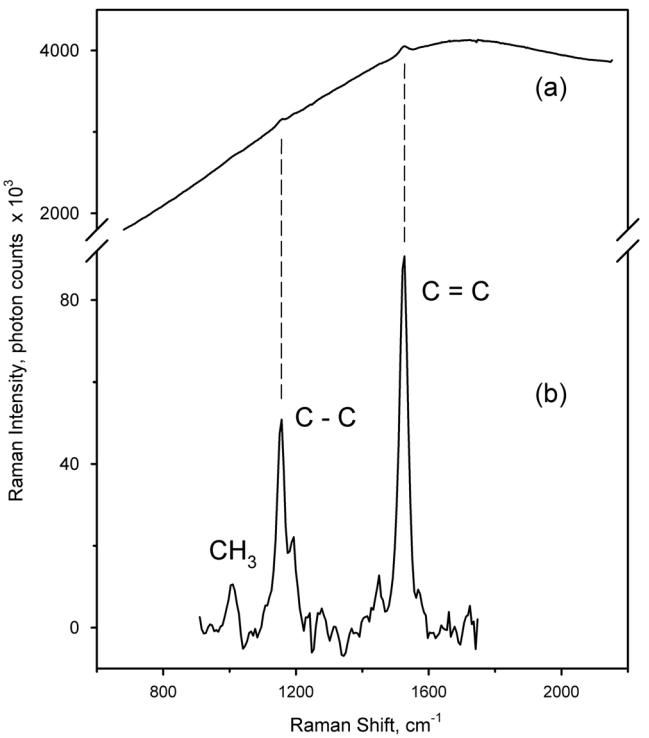

Fig. 2 (a) Fluorescence spectrum with superimposed sharp resonance Raman lines of excised human femoral spongy bone sample, obtained under excitation with 488-nm light. (b) Isolated resonance Raman spectroscopy (RRS) spectrum obtained after subtraction of fluorescence background, displayed with expanded intensity scale. Raman lines characteristic for carotenoids appear at 1008, 1125, and 1558 cm^{-1}. They correspond, respectively, to the rocking motions of the methyl side groups and stretch vibrations of carbon-carbon single (C—C) and double (C═C) bonds.

response with superimposed, weak, sharp, Raman lines, and Fig. 2(b) shows the isolated carotenoid RRS response obtained after fitting the smooth fluorescence background with a fourth-order polynomial, subtracting it from trace Fig. 2(a) and expanding it vertically on the intensity axis. All three major RRS lines characteristic for carotenoids are visible. These includes the Stokes lines at 1008 cm^{-1}, corresponding to the rocking motion of the molecules' CH_3 methyl side groups, the line at 1125 cm^{-1}, corresponding to the C—C single-bond stretch vibration, and the strongest line at 1558 cm^{-1}, corresponding to the C=C double-bond stretch vibration.[14] The intensity of the latter was used as a quantitative measure of all carotenoid subspecies present in the tissue, since all subspecies contribute to the Raman intensity through their common C=C backbone vibration.[14]

In Fig. 3, we show the RRS results for the trabecular femoral bone biopsies of 33 patients as a histogram. Carotenoid RRS levels vary significantly between samples/patients with a maximal-observed sixfold difference between subjects. Qualitatively, this intersubject variation is similar to the carotenoid concentration variations found in other tissues, such as in the macular region of the human retina or in skin, and is very likely correlated also, in this tissue, to differences in dietary habits, in uptake, in lifestyle factors, such as smoking, and other determinants.[10]

2.2 *Absorption Spectroscopy*

The availability of excised tissue samples offered the possibility to establish a direct correlation between RRS-derived bone carotenoid levels and concentrations of carotenoid extracts. For this purpose, we ground up small bone fragments with a pestle in a porcelain mortar under acetone, transferred the obtained fine slurry to a 0.5-in. diameter glass test tube filled with 4-ml acetone, and let the tube sit at room temperature for 30 min to allow heavier particles to precipitate at the bottom. Subsequently, 2 ml of the extract was collected from the top of the test tube with a syringe and placed in a fused silica cell for direct absorption measurements.

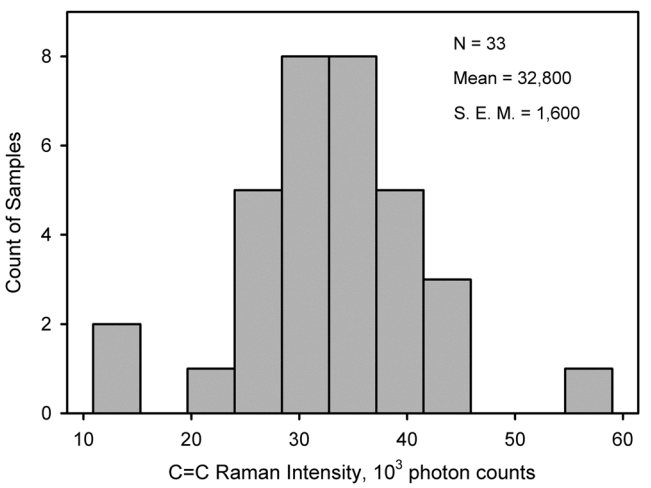

Fig. 3 Histogram of RRS intensities at the C=C stretch frequency obtained from 33 bone samples. Significantly, up to sixfold differences in bone carotenoid levels are apparent between samples. The envelope of the histogram suggests a bell-shaped curve for larger numbers of samples.

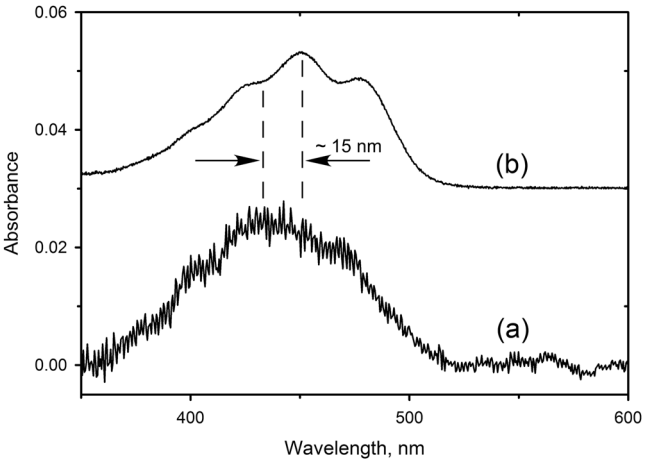

Fig. 4 (a) Absorption spectrum of acetone extract of femoral bone sample. (b) Absorption spectrum of pure β-carotene solution in acetone. Strong similarities exist in both spectra regarding the carotenoid absorption bands in the blue-green wavelength region near 440 nm including their characteristic vibronic sub-band structure; however, the absorption band is slightly shifted in bone to shorter wavelengths relative to the pure solution.

A typical absorption spectrum measured through such a bone carotenoid extract with 1-cm path length is shown in Fig. 4 and compared with the spectrum of a pure β-carotene solution measured with the same instrument. The raw absorption spectrum features a high-scattering background, which is due to the high concentration of lipids extracted from the bone marrow. After background subtraction, the remaining spectrum features an absorption band shifted by about 15 nm to shorter wavelengths with respect to pure β-carotene. In spite of the minor differences, these absorption results clearly confirm the presence of carotenoids in the extract and correspondingly in the bone samples. From the absorption strength of 0.024 optical density units at 435 nm for the sample of Fig. 4(a), measured over an optical path length of 1 cm, a total carotenoid concentration of 93 ng/mL in the extract and 1900 ng/g in the tissue can be estimated. Here, we approximate the extinction coefficient for bone carotenoids with that for β-carotene in petroleum ether solution, i.e., $A(1\%, 1\ \mathrm{cm}) = 2592$,[19] then use the expression

$$C = \frac{A}{A^{1\%}_{1\ \mathrm{cm}}} \cdot 10 \frac{\mathrm{mg}}{\mathrm{mL}}$$

for the calculation of the carotenoid concentration in solution, and finally obtain

$$C_B = \frac{C \cdot V}{m}$$

for the concentration in bone, where V is the volume of the extract (4 mL), and m is the mass of the bone sample (0.195 g) used for the preparation of the extract.

In agreement with the yellowish appearance of the bone samples, their concentrations appear to be higher than in skin, where an average of about 950 ng/g was found in 8 excised heel skin samples,[20] and an average of about 300 ng/g in 28 excised abdominal tissue samples.[21]

2.3 *High-Performance Liquid Chromatography*

The RRS detection method is sensitive only to the vibrations of the carbon backbone common to all carotenoid species and not to the molecular end groups. Therefore, it measures the integral optical response ("composite score") of all carotenoid species present in the measured tissue volume. In contrast, the biochemical gold standard detection technique of high-performance liquid chromatography (HPLC) is capable of detecting each individual carotenoid subspecies. To gain insight into the carotenoid composition of human bone and their relative abundance, we analyzed biopsied samples with the HPLC method as a next step.

To achieve high-detection accuracy (~15%), relatively large bone samples (~200 mg) were used. Following biopsy and weighing, the collected samples were immediately frozen until later HPLC analysis.[22] The protocol involved weighing the samples again, transferring them into tubes with 430-μl phosphate buffered saline (PBS) and 70-μL collagenase (70-mg/mL PBS), incubating them for 1 h at 37°C, and adding glass beads and a 2 mL mixture of 50% methanol/50% THF and 100 μL of tocol (internal standard). Further, the samples were mixed to macerate the tissue and to extract the carotenoids. Samples were saponified overnight at 4°C by the addition of 100-μL of 10% pyrogallol and 1 mL of 40% potassium hydroxide. Samples were extracted two times with 5-mL hexane and dried over sodium sulfate. The combined hexane extract was dried in a SpeedVac™. The sample for astaxanthin analysis was extracted with acetone rather than CH_3OH/THF and was hydrolyzed using cholesterol esterase. It was separated by HPLC using a Diol column.

The HPLC system consisted of a computer data system, an autosampler for maintaining samples at 20°C, a column heater at 31°C, and a diode array detector (ThermoSeparation Products, Fremont, California). The separation was performed isocratically on a Spherisorb ODS2 column (3 μm, 4.0 × 250 mm with titanium frits; ES Industries, West Berlin, New Jersey) protected by a Javelin™ guard column containing a similar stationary phase (Thermo Electron Corp., Bellefonte, Pennsylvania). The mobile phase consisted of acetonitrile/dioxane/isopropanol/triethylamine (80/15/5/0.1) at a flow rate of 1.0 mL/min. The alcohol component contained 100-mM ammonium acetate. The diode array detector with light pipe flow cell was programmed to monitor tocol and phytoene at 290 nm, phytofluene at 325 nm, and carotenoids at 450 nm.

Linear calibration curves were prepared for three concentrations of analytes, which spanned the physiological levels of micronutrients in serum. The calibrants included are astaxanthin, lutein, zeaxanthin, α-cryptoxanthin, β-cryptoxanthin, lycopene, α-carotene, β-carotene, phytoene, and phytofluene.

A typical HPLC chromatogram of a biopsied bone sample is shown in Fig. 5, demonstrating good signal-to-noise ratios for all carotenoid peaks and allowing us to determine their individual concentrations in bone with high accuracy. Importantly, a wide spectrum of carotenoids in bone is apparent including lutein, zeaxanthin, α- and β-cryptoxanthins, *trans*- and *cis*-lycopene, α-carotene, *trans*- and *cis*-β-carotene, phytoene, and phytofluene.

To further establish a correlation between optically and biochemically derived tissue carotenoid content, and in this way to validate a quantitative optical detection approach, we selected nine biopsied samples with low-, medium-, and high-carotenoid contents, respectively, as determined via RRS measurements, and subsequently determined their carotenoid content via

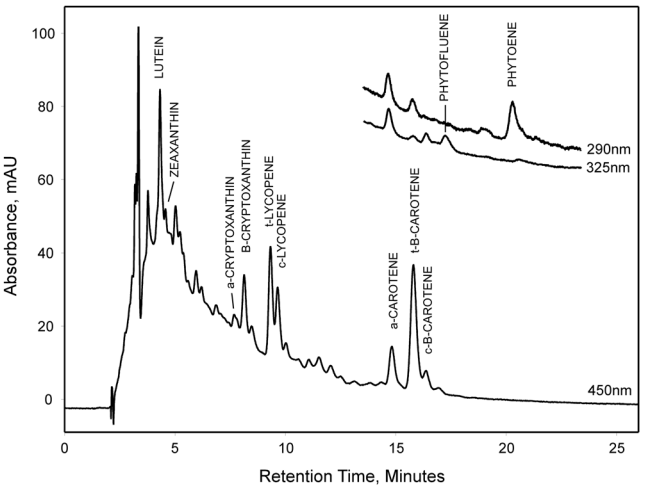

Fig. 5 HPLC chromatogram of excised femoral bone sample extract, proving the existence of about a dozen carotenoid species in bone, including their isomers. Data here were obtained measuring absorption at 450 nm. All carotenoids known to exist in human serum are present also in the bone sample. Carotenoids with highest abundances are lutein, the cryptoxanthins, carotenes, and lycopene. Inset shows HPLC data obtained with absorbance measurements at 290 and 325 nm, demonstrating also the presence of phytofluene and phytoene.

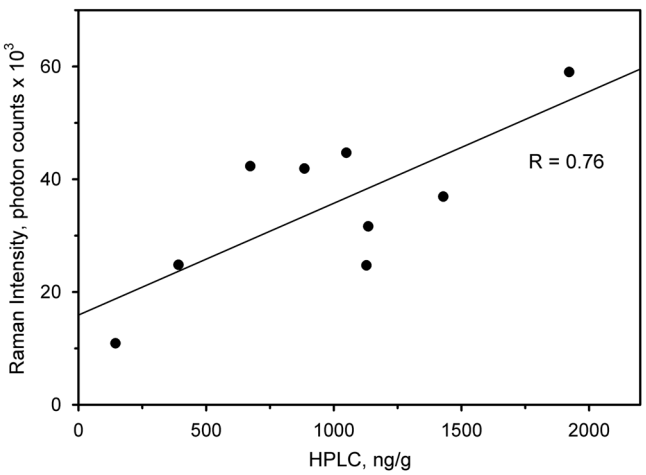

Fig. 6 Plot of Raman- and HPLC-derived bone carotenoid levels for nine different samples, demonstrating high correlation between optical and biochemical detection methods (with correlation coefficient $R = 0.76$).

HPLC analysis. The results are shown in Fig. 6, yielding a satisfactory high-correlation coefficient of ~0.76. The blue-light excitation RRS measurements are not sensitive to phytoene and phytofluene, which due to their relatively short conjugation lengths absorb at much shorter wavelengths in the UV.[15] In calculating the total carotenoid content by HPLC, their respective concentrations were subtracted.

The obtained correlation between optically and biochemically derived bone carotenoids is surprisingly high in view of the fact that bone tissue provides a rather heterogeneous light-tissue interaction scenario. Bone morphology and light propagation are conceptually illustrated in Fig. 7. It shows idealized cross-sections through extreme cases of healthy and osteoporotic spongy bone samples, respectively, on a millimeter-scale spatial resolution, with the laser light excitation area inside the bone tissue indicated as a shaded hemisphere. The light

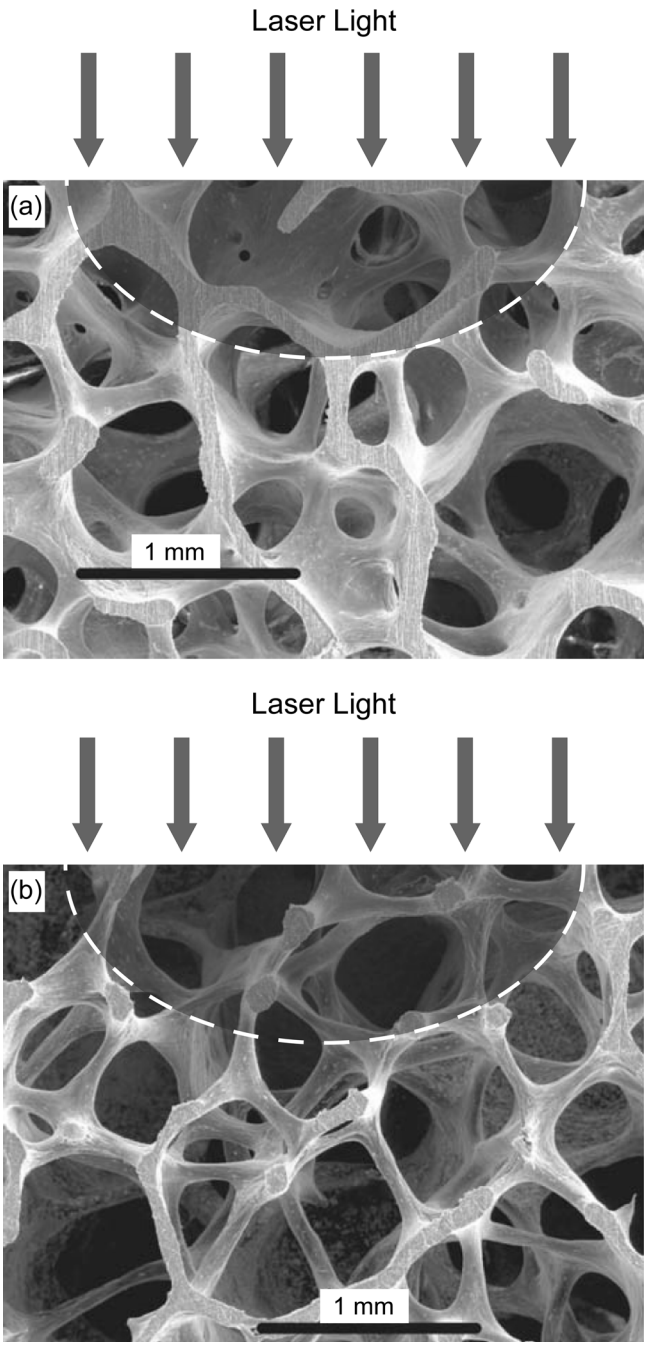

Fig. 7 Conceptual illustration of light-tissue interaction in bone. Structures of spongy bones for (a) a healthy subject and (b) a subject with degraded bone health show a noticeable difference in thicknesses of bone trabeculae between subjects. The light excitation disks inside the bone are indicated with a white boundary. The excitation light encounters carotenoid-containing bone marrow inside the trabecular spaces as well as carotenoid-free trabecular walls. Images of bone structure adapted from Ref. 23.

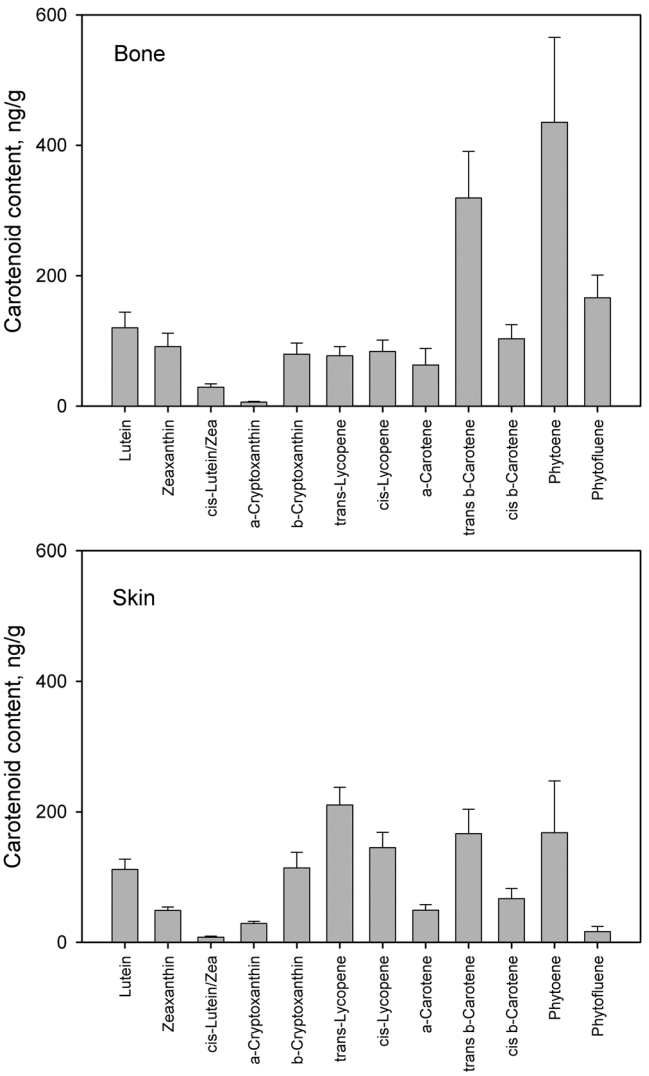

Fig. 8 Comparison of carotenoid levels for excised femoral bone and skin samples, which is shown as two histograms for nine and eight samples, respectively. Note the similarities in abundance of particular carotenoid species (e.g., lutein and zeaxanthin versus β-carotene levels). Lycopene levels appear to be lower in bone relative to skin. Error bars indicate standard error of the mean for each carotenoid species.

excitation encounters carotenoid-containing bone marrow located inside the spongy bone cavities as well as their carotenoid-free calcium walls. The wall thicknesses are known to vary between patients, thinning considerably in patients with osteoporosis, for example. As a consequence, the morphological bone differences between subjects will lead to differences in the spatial overlap of the light excitation and the carotenoid-containing soft tissue (marrow) mass located inside the cavities and influence the obtainable correlation between optically and biochemically determined bone carotenoid content.

All carotenoids found in human skin[24] apparently exist also in human spongy bone. To illustrate this point more quantitatively, we show in Fig. 8 the relative abundances of carotenoids measured via HPLC analysis in nine excised bone and eight skin samples, respectively, with samples originating from different subjects. In bone, the concentrations of lutein, zeaxanthin, and β-crytoxanthin appear to be similar to skin, while the concentrations of carotene, phytoene and phytofluene appear to be higher (up to a factor of 2). Potentially these tissue differences could be important, but a larger number of samples/subjects are needed for sufficient statistical power.

2.4 *Reflection Spectroscopy*

While RRS spectroscopy is well suited for the detection of carotenoids with high-molecular specificity and, in principle, can also be used in filter-based spatial imaging configurations, its

implementation is rather complex, requiring relatively complicated 488-nm laser excitation with sequential detection on and off the Raman line.[25] A potentially much simpler methodology for the remote optical detection of bone carotenoid status during total knee arthroplasty is reflection-based imaging. To develop this methodology for bone carotenoid detection, we first measured reflection spectra of bone and surrounding tissue in a spectrally resolved nonimaging configuration to determine if the characteristic yellow tissue colorations due to carotenoids can be quantified with sufficient sensitivity. As a setup, we used broadband white light illumination over the 380 to 750-nm spectral range in combination with a spectrograph/CCD array detection system, analyzing the light that is reflected back from the sample in 180-deg back-reflection geometry. Essentially, the setup is the same as previously used for the measurement of carotenoids in human skin.[26] The apparent absorbance, A, of the sample is calculated as $A = -\lg(R/100)$ for each spectral data point, where R is the measured reflectivity.

In Fig. 9, reflection-derived apparent absorption spectra in the 380 to 750-nm spectral range are shown for excised spongy bone, fat, and cartilage samples. For the bone and fat samples, strong carotenoid vibronic absorption bands are clearly discernible, superimposed on a scattering background, at ~450 and 480 nm, with potentially interfering tissue chromophores largely absent. In cartilage, no carotenoids are detectable. The concentration of hemoglobin differs between tissues types, as can be seen from differences in its characteristic single-band absorption strength at ~420 nm and its double-band absorption structure at ~560 nm.

The apparent absorption spectra of spongy bone and fat samples exhibit nearly identical combined absorption and scattering behaviors in the red spectral region between 600 and 750 nm, as can be seen from Fig. 10. This spectral region can therefore be used as an effective background absorption/scattering level for the calculation of carotenoid levels from their absorption in the blue spectral region. Absorbance differences in the spectral range from ~450 to 520 nm would then correlate with different tissue carotenoid concentrations. Spectral regions suitable for quantitative reflection-based imaging of carotenoid levels in spongy bone and fat tissues are indicated in Fig. 10 as "carotenoid detection band" and "reference band," respectively. The spectral location of the reference band is chosen to avoid potential absorption overlap from confounding chromophores, such as hemoglobin, and at the same time to provide a measure for the scattering background that is comparable with the scattering background under the "carotenoid detection band."

To prove this concept, we constructed a filter-based reflection imaging setup, which is shown schematically in Fig. 11. Light from a spectrally broad "white" light emitting diode (LED) is routed to the surface of the tissue sample with the help of a simple lens projection configuration. The overall excitation light power of the LED was about 5 mW, corresponding to an excitation light intensity of ~80 μW/cm^2. The light scattered back from the tissue is collected by an objective lens and transmitted sequentially through two band-pass filters with peak transmissions at 620 and 488 nm, respectively, mounted on a filter wheel. The bandwidths of the transmitted light were 10 nm in both cases. The spectrally filtered images were recorded with the 512×512 pixel array of a CCD camera (Santa Barbara Instrument Group, Santa Barbara, CA, Model ST-9; pixel size 20×20 μm), permitting digital image acquisition with 16 bits of grayscale. The camera was positioned about

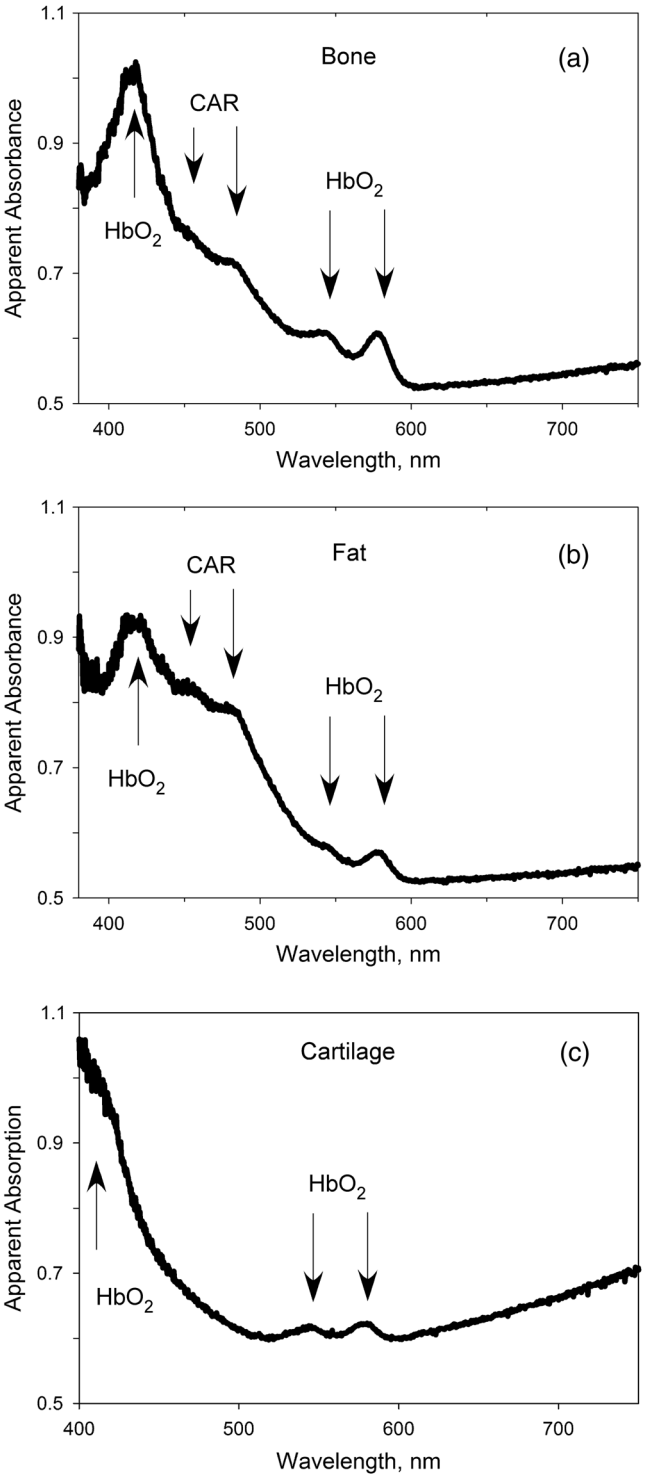

Fig. 9 Apparent absorption spectra of (a) spongy bone, (b) fat, and (c) cartilage-excised tissue samples measured in the spectral range of 380 to 750 nm with diffuse reflection spectroscopy. The presence of hemoglobin in all tissues types (in different relative amounts) is evident due to its characteristic single-band absorption at ~420 nm and double band absorption structure at ~560 nm. For the bone and fat samples, carotenoid vibronic absorption bands are clearly discernible at ~450 and 480 nm above the scattering background.

40 cm from the object plane, thus viewing the samples with a 29-deg field-of-view.

For the generation of bone carotenoid reflectivity maps and corresponding optical densities, we first recorded a "red" tissue

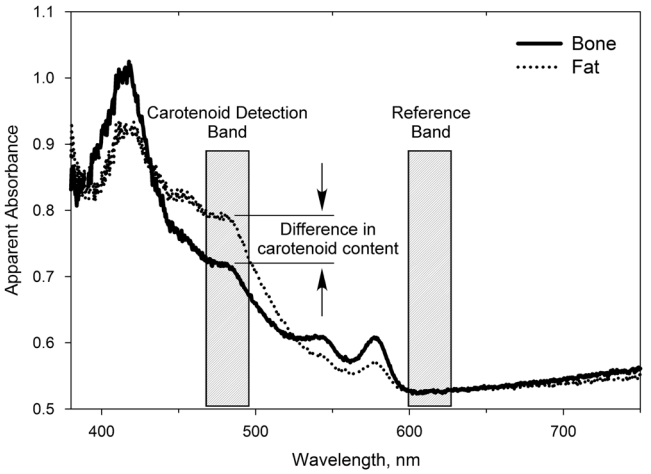

Fig. 10 Apparent absorption spectra of spongy bone and fat samples exhibit similar absorption behavior in the red spectral region between 600 and 750 nm. This region can be used as a background reference for the calculation of carotenoid levels. Absorbance differences in the spectral range from ~450 to 520 nm would be due to different tissue carotenoid concentrations.

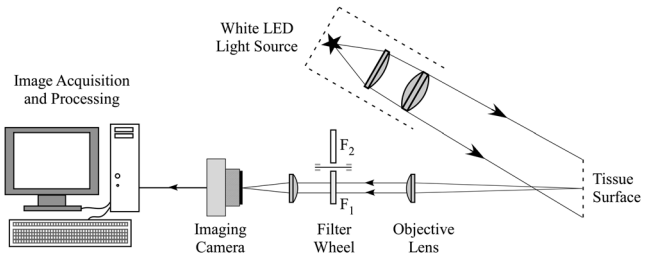

Fig. 11 Schematic description of reflection-imaging method for biopsied samples or exposed living tissue, consisting of a white-light source with broad-spectral emission range that overlaps the absorption regions of interest, reflected light collection lens, spectrally resolved detection with filters and CCD camera, image acquisition, and data-processing electronics.

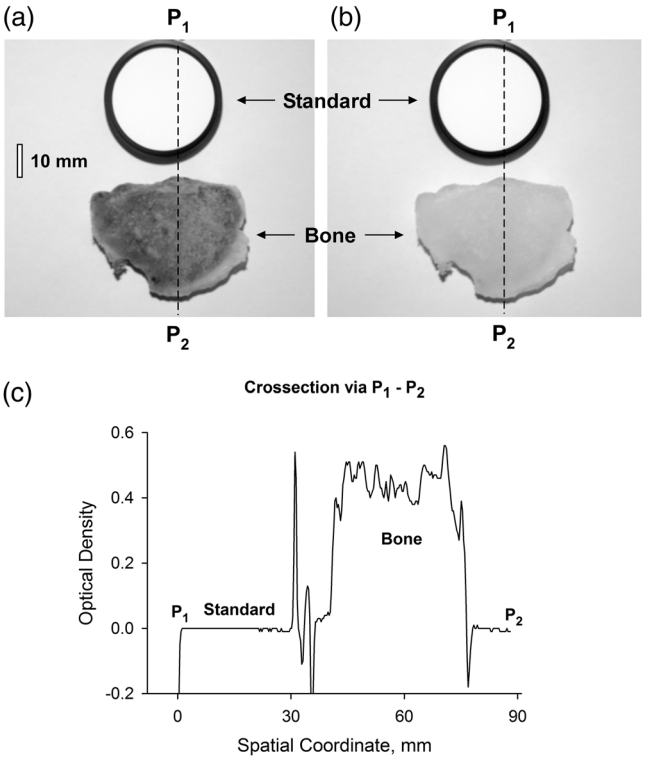

Fig. 12 Spectral imaging results of excised bone samples obtained with setup of Fig. 11. (a) Images of a white reflection standard and spongy bone sample obtained, respectively, when selectively recording/filtering out only the "carotenoid detection band," i.e., the ~475 to 495-nm spectral region. (b) Corresponding images for the same white standard and bone sample when selectively recording/filtering out only the "reference band," i.e., the ~600 to 620-nm spectral region. (c) Spatially resolved line plot of the apparent optical density of the bone carotenoid levels across image points P_1–P_2, obtained by taking the difference of the common logarithms of the corresponding normalized image pixel intensities along the P_1–P_2 direction. Note the high-carotenoid optical density levels of the spongy bone sample of about 0.5 over most of its central surface.

image along with an image of a reflection standard ("Spectralon," Labsphere, Inc., North Sutton, NH) placed in the same object plane [see Fig. 12(a)]. Subsequently, we normalized each red tissue image pixel to the reflection standard and calculated the common logarithm according to

$$F_i^r = -\log_{10}\left(\frac{I_i^r}{I_0^r}\right),$$

where I_i^r is the intensity of the pixel number i under red detection, and I_0^r is the average intensity over the white standard. A similar procedure was used for the generation of a "blue" reflectivity map of the sample after exchange of the filter, resulting in an optical density map

$$F_i^b = -\log_{10}\left(\frac{I_i^b}{I_0^b}\right).$$

Subsequently, the two optical density maps can be subtracted to generate pixel line plots across directions of interest, such as through the center of the sample, as shown in Fig. 12(c) for a spongy bone sample exhibiting carotenoid levels as high as 0.5 optical density units on average over most of its central surface.

Importantly, this reflection imaging-derived concentration is about the same as the concentration derived via direct absorption measurement of the extract, according to Fig. 4 (estimating an effective path length of ~0.5 mm for reflection in the blue wavelength region in the bone and taking into account the 1 cm path length in the extract).

3 Discussion

Our results show that carotenoids exist in human bone and surrounding fatty tissue in high concentrations and in the same variety of subspecies found in skin and they are known to circulate in the blood stream. Carotenoid levels can be detected quantitatively in exposed bone and surrounding tissue in noncontact detection configurations using RRS. A proof of concept experiment shows that reflection spectroscopy could be a viable alternative. Its implementation is relatively simple, essentially requiring only spectrally selective, filter-based photography, and it can generate spatially resolved quantitative information on tissue carotenoid levels. The method would therefore be applicable in clinical settings where exposed tissues could be measured during surgery, such as in total knee arthroscopy.

Measuring or estimating the carotenoid levels of a patient's bones or surrounding tissue provide many potential benefits.[27]

For example, the patient and doctor can be better guided in selecting an appropriate bone integration implant device (e.g., cemented implant devices may be more appropriate when bone carotenoid levels are low). Similarly, if a patient's bone carotenoid content is known or estimated to be low, the patient can be encouraged to make dietary changes (e.g., consuming carotenoid-rich foods and/or carotenoid nutraceuticals) or to select medical regimens for improving bone health (e.g., combining prescription drugs with exercise regimens and nutritional changes). Further, a known or measured bone carotenoid level may be used to predict the health of other organs or systems (e.g., cardiovascular health, neurologic health, mental health, eye health, insulin sensitivity, etc.).

Since the carotenoid species found in bone are similar to skin, it may be possible to establish skin carotenoid measurements as a surrogate marker for these internal tissues. A clinical trial is under way to investigate a likely correlation between the carotenoid concentration of a patient's exposed bone tissue with skin, which can be more easily assessed optically. A resulting correlation table could be particularly useful when a patient's carotenoid concentrations are optically tracked over time.

Currently, in orthopedic surgery, there is much discussion and disagreement on the relative advisability and durability of knee, hip, and shoulder implants either as cemented by methyl methacrylate or press fit (cement-less) for direct bone integration.[28] Press-fit knee implants achieving successful bone integration and bonding are often recommended for 50- to 70-year-old patients. However, many surgeons remain reluctant to use press-fit implants for fear of unsuccessful bone integration. This study looks at measuring the relative concentration of carotenoids exposed during routine bone cuts as a possible predictor of bone health and therefore a predictor of robust bone integration and bonding.

References

1. N. I. Krinsky, S. T. Mayne, and H. Sies, Eds., *Carotenoids in Health and Disease*, Marcel Dekker, New York, NY (2004).
2. D. S. Michaud et al., "Intake of specific carotenoids and risk of lung cancer in 2 prospective US cohorts," *Am. J. Clin. Nutr.* **72**(4), 990–997 (2000).
3. M. Zhang, C. D. Holman, and C. W. Binns, "Intake of specific carotenoids and the risk of epithelial ovarian cancer," *Br. J. Nutr.* **98**(1), 187–193 (2007).
4. E. Giovannucci et al., "Intake of carotenoids and retinol in relation to risk of prostate cancer," *J. Natl. Cancer Inst.* **87**(23), 1767–1776 (1995).
5. L. Le Marchand et al., "Intake of specific carotenoids and lung cancer risk," *Cancer Epidemiol. Biomarkers Prev.* **2**(3), 183–187 (1993).
6. L. Wang et al., "Associations of plasma carotenoids with risk factors and biomarkers related to cardiovascular disease in middle-aged and older women," *Am. J. Clin. Nutr.* **88**(3), 747–754 (2008).
7. Age-Related Eye Disease Study Group, "The relationship of dietary carotenoid and vitamin A, E, and C intake with age-related macular degeneration in a case-control study: AREDS Report No. 22," *Arch. Ophthalmol. (Chicago)* **125**(9), 1225–1232 (2007).
8. A. L. Ray et al., "Low serum selenium and total carotenoids predict mortality among older women living in the community: the women's health and aging studies," *J. Nutr.* **136**(1), 172–176 (2006).
9. S. T. Mayne et al., "Noninvasive assessment of dermal carotenoids as a biomarker of fruit and vegetable intake," *Am. J. Clin. Nutr.* **92**(4), 794–800 (2010).
10. S. T. Mayne et al., "Resonance Raman spectroscopic evaluation of skin carotenoids as a biomarker of carotenoid status for human studies," *Arch. Biochem. Biophys.* **539**(2), 163–170 (2013).
11. M. Yamaguchi, "β-cryptoxanthin and bone metabolism: the preventive role in osteoporosis," *J. Health Sci.* **54**(4), 356–369 (2008).
12. M. Sugiura et al., "Bone mineral density in post-menopausal female subjects is associated with serum antioxidant carotenoids," *Osteoporos. Int.* **19**(2), 211–219 (2008).
13. S. Sahni et al., "Protective effect of total carotenoid and lycopene intake on the risk of hip fracture: a 17-year follow-up from the Framingham osteoporosis study," *J. Bone Miner. Res.* **24**(6), 1086–1094 (2009).
14. I. V. Ermakov et al., "Resonance Raman detection of carotenoid antioxidants in living human tissues," *Opt. Lett.* **26**(15), 1179–1181 (2001).
15. I. V. Ermakov et al., "Resonance Raman detection of carotenoid antioxidants in living human tissue," *J. Biomed. Opt.* **10**(6), 064028 (2005).
16. I. V. Ermakov et al., "Application of resonance Raman spectroscopy to the detection of carotenoids in vivo," in *Carotenoids—Physical, Chemical and Biological Functions and Properties*, J. T. Landrum, Ed., pp. 87–109, CRC Press, Atlanta (2009).
17. M. V. Schulmerich et al., "Transcutaneous Raman spectroscopy of murine bone in vivo," *Appl. Spectrosc.* **63**(3), 286–295 (2009).
18. M. D. Morris, "Raman spectroscopy of bone and cartilage," Chapter 13 *Emerging Raman Applications and Techniques in Biomedical and Pharmaceutical Fields*, P. Matousek and M. D. Morris, Eds., pp. 347–364, Springer Verlag, Berlin (2010).
19. G. Britton, "UV and visible spectroscopy," in *Carotenoids: Spectroscopy*, G. Britton et al., Eds., Vol. 1B, pp. 13–63, Birkhauser Verlag, Basel (1995).
20. I. V. Ermakov and W. Gellermann, "Validation model for Raman based skin carotenoid detection," *Arch. Biochem. Biophys.* **504**(1), 40–49 (2010).
21. S. T. Mayne et al., "Noninvasive assessment of dermal carotenoids as a biomarker of fruit and vegetable intake," *Am. J. Clin. Nutr.* **92**(4), 794–800 (2010).
22. N. E. Craft and H. C. Furr, "Improved HPLC analysis of retinol and retinyl esters, tocopherols, and carotenoids in human serum samples for the NHANES," *FASEB J.*, **367.11**, A534 (2004).
23. R. O. Ritchie, M. J. Buehler, and P. Hansma, "Plasticity and toughness in bone," *Phys. Today* **62**(6), 41–47 (2009).
24. Y. M. Peng et al., "Concentrations and plasma-tissue-diet relationships of carotenoids, retinoids, and tocopherols in humans," *Nutr. Cancer* **23**(3), 233–46 (1995).
25. M. Sharifzadeh et al., "Resonance Raman imaging of macular pigment distributions in the human retina," *J. Opt. Soc. Am.* **25**(4), 947–957 (2008).
26. I. V. Ermakov and W. Gellermann, "Dermal carotenoid measurements via pressure mediated reflection spectroscopy," *J. Biophotonics* **5**(7), 559–570 (2012).
27. J. W. Smith et al., "Significance of C-reactive protein in osteoarthritis and total knee arthroplasty outcomes," *Ther. Adv. Musculoskelet. Dis.* **4**(5), 315–325 (2012).
28. G. Demey et al., "Cemented versus uncemented femoral components in total knee arthroplasty," *Knee Surg. Sports Traumatol. Arthrosc.* **19**(7), 1053–1059 (2011).